Comparison of Traditional and Newly Developed Thunderstorm Indices for Switzerland

H. HUNTRIESER, H. H. SCHIESSER, W. SCHMID, AND A. WALDVOGEL

Institute of Atmospheric Science, Swiss Federal Institute of Technology, Zurich, Switzerland

(Manuscript received 21 August 1995, in final form 26 June 1996)

ABSTRACT

The preconvective environment on thunderstorm days in Switzerland north of the Alps has been investigated during a 5-yr period (1985–89). Thermodynamic and kinematic parameters calculated from the radiosounding in Payerne (started at 0000 and 1200 UTC) were used to characterize the initiation of convection. The best parameters were evaluated by using three methods: 1) skill scores, 2) probability distributions, and 3) mean temperature soundings and hodographs. For the decision whether a thunderstorm day was expected or not, the best results were obtained at 0000 UTC with the original Showalter index and at 1200 UTC with the SWEAT index. In addition, to decide whether an isolated or widespread thunderstorm day was expected, the most successful parameter was the modified $CAPE_{CCL}$. Furthermore, the best thermodynamic and kinematic parameters were combined to create new thunderstorm indices, similar to the calculations of the SWEAT index in the United States. The new thunderstorm indices especially designed for northern Switzerland were jointly called the ''SWISS index'' (combined stability and wind shear index for thunderstorms in Switzerland). All of the traditional and new indices were verified with independent data from 3 yr (1990, 1992, and 1993), showing the best results for the new combined indices.

1. Introduction

Concern about the environment, including natural disasters and climate changes, has increased significantly during the last decade. Thunderstorms are a major cause of natural disasters in the alpine region (Fig. 1) during the summer season. Despite all of these well-known observations, the investigation of the preconvective environment of thunderstorms has been neglected in Europe in comparison to the United States where in general more severe thunderstorms occur (Newton 1967; Modahl 1979; Wilson and Schreiber 1986; Rockwood and Maddox 1988; Johns and Doswell 1992; Mueller et al. 1993; Fuelberg and Biggar 1994). Analyses of the behavior of thunderstorms in Switzerland are important, since the alpine area of Switzerland (Fig. 1) belongs to the most preferred regions in Europe for the initiation of thunderstorms (Collier and Lilley 1994).

The general preconditions for the initiation of thunderstorms are well known and have been summarized by, for example, Doswell (1987) and Johns and Doswell (1992): 1) conditional instability, 2) a moist layer of sufficient depth in the lower or midtroposphere, and 3) a source of lift to initiate the convection. The formation of thunderstorms is an interaction between these conditions on different scales (Doswell 1987): ''It is proposed that convective systems depend primarily on large-scale processes for developing a suitable thermodynamic structure, while mesoscale processes act mainly to initiate convection.'' Hence, it follows that thunderstorms can be initiated by mesoscale processes even when the synoptic conditions are not ideal. However, the intensification or further development of these thunderstorms on a large scale is unlikely.

Forecasting thunderstorms is one of the most difficult tasks in weather prediction, due to their rather small spatial and temporal extension (Orlanski 1975) and due to the lack of horizontal and vertical resolution of the operational numerical models (Anthes 1976; Lilly 1990). Therefore, a variety of different thermodynamic and kinematic parameters have been derived from sounding data during the past 40 yr (see the appendix). Each of them indicated the thunderstorm potential of an air mass (Peppler and Lamb 1989). Studies on the efficiency of different stability indices for the thunderstorm prediction have been presented by several authors, for example, Neumann (1971), Anthes (1976), Reap and Foster (1979), Stone (1985), Andersson et al. (1989), Schultz (1989), Jacovides and Yonetani (1990), and Lee and Passner (1993). Additionally, one of the above-mentioned authors (Schultz 1989) comments: ''However, there have been relatively few studies of the behavior and the relative effectiveness of the various indices. This

Corresponding author address: Ms. Heidi Huntrieser, Institut fuer Physik der Atmosphaere, DLR Oberpfaffenhofen, Postfach 1116, D-82230 Wessling, Germany.
E-mail: heidi.huntrieser@dlr.de

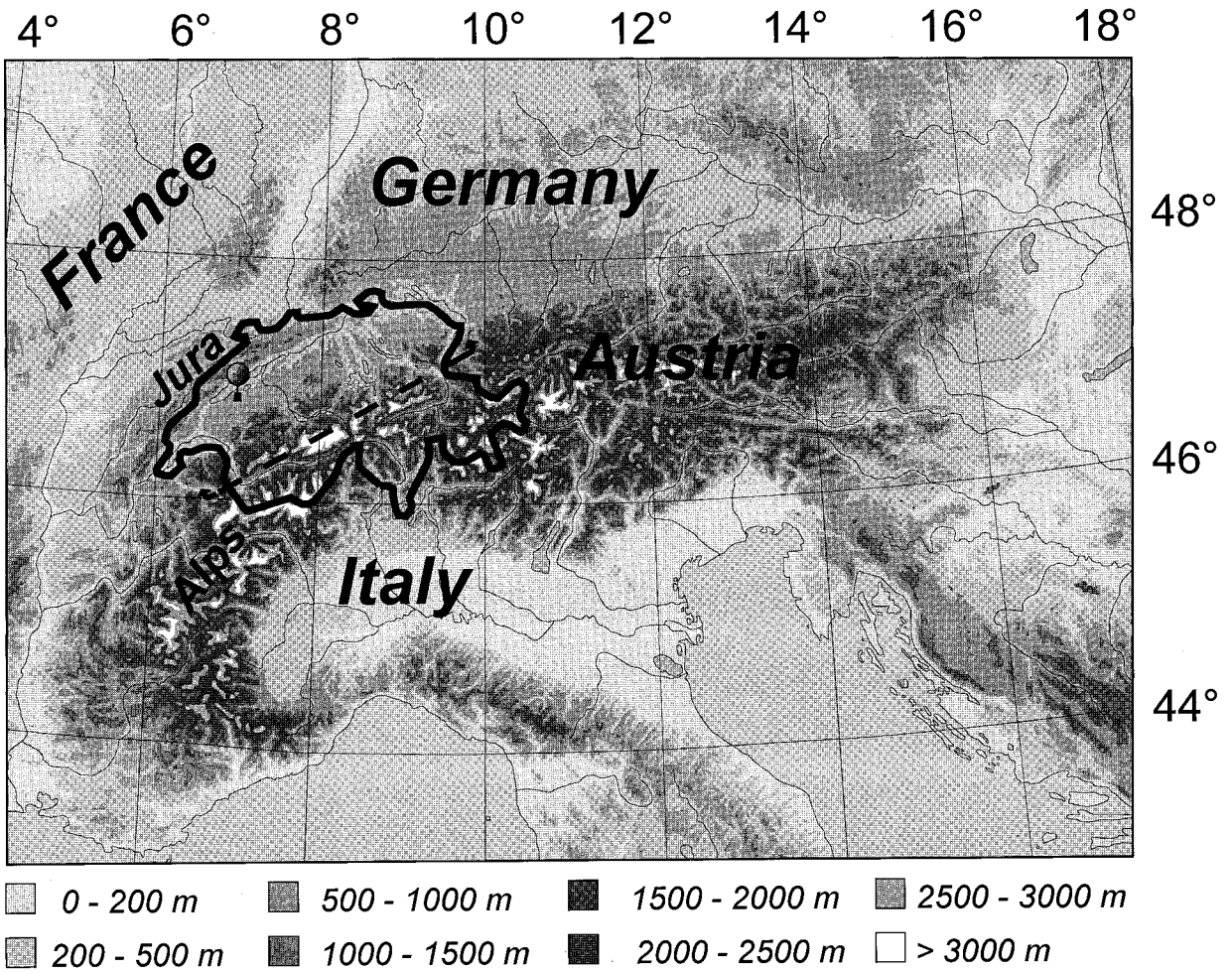

FIG. 1. Topographic view over the European alpine region with Switzerland (bold border) in the left center surrounded by France, Germany, Austria, and Italy. Two major mountain chains range over Switzerland: the Jura Mountains in the northwest and the Alps in the south. The bold dotted line with the arrows indicates the test area used in this study: the northern part of Switzerland. The only radiosonde site in Switzerland (Payerne) is marked with a balloon.

is unfortunate, because in addition to providing practical information to field forecasters, these studies invariably result in useful insights into the physical characteristics of thunderstorms and their environments.'' The present study tries to give some useful insights into the physical characteristics of thunderstorms and their prefered environments in Switzerland. The improvement of the thunderstorm prediction is important, especially for the prevention of injuries to people and damaged cars in contrast to the more unavoidable damages of buildings and in agriculture.

The state of the meteorological observation material in Switzerland has now reached a point that makes it possible to perform studies of thunderstorm environments comparable to studies from the United States. The aim of this paper is to investigate the relationship of different thermodynamic and kinematic parameters to the initiation of thunderstorms in Switzerland. This has been done by considering radiosounding data, data from a lightning detection network, and reports of hail damage from the Swiss Hail Insurance Company (see section 3). First the traditional stability indices presented in the appendix are tested for the thunderstorm prediction in northern Switzerland (see section 4). The results of these tests and the calculation of mean temperature soundings and hodographs for different days with no, isolated, and widespread thunderstorms over a 5-yr period (1985–89) lead to the development of new thunderstorm indices especially adjusted to the conditions in northern Switzerland: the so-called SWISS (stability and wind shear index for thunderstorms in Switzerland) indices (see section 5).

The aim and the content of the present study have many similarities to a recently presented paper by Fuelberg and Biggar (1994) about the preconvective environment of summer thunderstorms over the Florida panhandle. However, they have examined a smaller dataset from two summers (1990 and 1991) and compared only

five different stability indices [TT, K, SLI (surface lifted index), SI_{850}, and LI (lifted index)]. No new thunderstorm indices were developed for the investigated area.

2. Severe thunderstorms in Switzerland

Studies dealing with severe thunderstorms in Switzerland are quite rare. A climatological study of the mesoscale structure of severe precipitation events by using radar information has been published recently by Schiesser et al. (1995). The results show that about 40% of the mesoscale convective systems were moving into Switzerland from the west or southwest, while the rest of the systems were initiated within the borders of Switzerland. Most thunderstorms (66%) formed over western Switzerland. Less common was the formation of thunderstorms in the central and eastern parts of Switzerland (15%). The mature stage of the severe thunderstorms was observed most frequently in the central parts of Switzerland along the foothills of the Alps.

The characteristics of 42 severe hailstorms observed during an international field project ''Grossversuch IV'' (1977–82) in central Switzerland have been investigated by Houze et al. (1993). The hodographs in the environment of these storms showed wind shear values just about one-half to two-thirds of the values associated with supercell storms over the central United States. The Swiss wind shear vector generally veers clockwise with height through the lowest 5–6 km with a tendency for a lower-tropospheric southwesterly jet at the 700-hPa level. In comparison this jet is observed at the 850-hPa level in the U.S. cases. The clockwise veering of strong lower-tropospheric wind shear (associated with warm air advection) accounts for the predominance of right-moving hailstorms (Rotunno and Klemp 1982) as observed over the central United States. In contrast, Houze et al. (1993) observed that the Swiss hailstorms are nearly equally divided between left- and right-moving storms. The reason for this equal division was attributed to orographical effects on the local airflow in the region where the storms developed. Houze et al. (1993) also found that the values of convective available potential energy (CAPE) (see the appendix) are quite variable for the observed storms during Grossversuch IV, reaching from 340 to 2340 J kg^{-1}. The CAPE values tend to be smaller on average than similar values associated with supercellular storms in the central United States, which may exceed 2500 J kg^{-1}.

The most severe Swiss hailstorms nevertheless have significant features of supercell storms (Schmid et al. 1993). The updraft rotation accompanying supercell storms is believed to be generated by the stretching and tilting of streamwise vorticity associated with the environmental wind shear (Davies-Jones 1984; Rotunno and Klemp 1985). In a recent study presented by Schmid and Huntrieser (1994) the wind field in the environment of supercell storms in Switzerland was investigated. The results show the presence of substantial wind shear and helicity (Lilly 1986) in the vicinity of Swiss supercell storms. Helicity is on the order of 100–200 m^2 s^{-2}, which means that the ''streamwise vorticity'' hypothesis suggested by Davies-Jones (1984) is a reasonable explanation for the observed vortex signatures (Moller et al. 1994).

Recently, Huntrieser et al. (1994a,b) and Huntrieser (1995) analyzed the synoptic and mesoscale environment of the most severe Swiss hail days since 1950. The most common features of these severe cases can be summarized as follows: 1) ''low-index'' situation, 2) trough or cut-off low over the Bay of Biscay, 3) on the leeward side of the trough is a shallow depression located over France, 4) the associated cold front extends far southward and separates the maritime subtropical air from the maritime polar air, 5) in the warm sector of the depression the warm and moist air from the Iberian Peninsula [''Spanish plume,'' see Morris (1986)] is transported to central Europe with southwesterly winds, 6) at the same time cold advection in high altitudes becomes apparent with the approach of the trough, 7) the result is a distinct increase of instability, 8) especially strong thunderstorm developments are to be expected if the cold front reaches Switzerland in the late afternoon or evening, and 9) $CAPE_{CCL} > 600$ J kg^{-1} and the vertical wind shear of the lowest 6 km exceeds 5 m s^{-1} per 6 km (see the appendix).

3. Method

a. Definition of thunderstorm days

This study includes thunderstorm days north of the Alps in Switzerland. The observation area is indicated in Fig. 1 between the bold dashed line with the arrows and the northern border of Switzerland. Thunderstorms have been studied during a 5-yr period (1985–89) from May to August (615 days).

An automatic mesoscale network (ANETZ) operated by the Swiss Meteorological Institute (SMI) delivers meteorological data with a temporal and spatial resolution of 10 min and 20–25 km, respectively, since 1978. The 36 weather stations in the observation area are supplied with lightning counters that record the near ($\leq$5 km) and distant (5–25 km) lightning sum for each hour. The reports of hail damage from the Swiss Hail Insurance Company are also useful for thunderstorm statistics. From each community in Switzerland with insured agriculture, each single day with hail damage is reported to the insurance company. The communities in the observation area are small and cover an area of $\sim$10 km^2 on average. In addition the operational radar images produced by the SMI contain information about the occurrence of thunderstorms. These images have a temporal and spatial resolution of 10 min and 2 km $\times$ 2 km, respectively.

To determine the thunderstorm days in the observation area, lightning reports were used in addition with

hail damage reports to determine the most severe thunderstorm days. From the range and the spatial resolution of the lightning counters it is assumed that nearly each thunderstorm occurring in the observation area is registered. A comparison between the radar images (criterion for a thunderstorm day: occurrence of a radar echo of at least 47 dBZ = 30 mm h^{-1} rainfall intensity) and the lightning reports (near and distant) was carried out at the beginning of the investigations using 4 months of data, which resulted in almost the same sample of defined thunderstorm days when using the near lightning reports (Huntrieser 1995). In comparison distant lightning reports were sometimes false due to corona discharges near the mountain peaks, and three reporting stations had to be excluded from the study. Finally, the near lightning reports from 33 ANETZ stations were considered for the investigation. Since no radar images were available for the southern part of Switzerland during the investigation period, no comparison with the lightning reports from the ANETZ stations in this area was possible. Therefore, this part of Switzerland was excluded from this study.

In this study it is assumed that the radiosounding in Payerne represents the preconvective conditions over the whole observation area (~250 km × 100 km). A further assumption is that both daily radiosoundings (from 0000 and 1200 UTC) must represent the daily preconvective situation. This criterion can only be fulfilled if the thunderstorms occurring during the afternoon (1240–2340 UTC, first and last lightning counts) are considered. During this time period about 80% of the radar detected severe hail cells occurred during the years 1983–94 (Gruppe für Radarmeteorologie 1995). Days with thunderstorms before 1240 UTC are excluded from the study because the 1200 UTC radiosounding is no longer representative of a preconvective environment. Without this criterion, neither daily radiosoundings is available for a comparison. Days with incomplete soundings (e.g., when wind data were missing or when the sounding was interrupted too early) were also excluded. Altogether the original dataset (615 days) was reduced by 99 days. The remaining 516 days were then divided into (a) days without thunderstorms: no ANETZ stations have reported near lightnings between 1240 and 2340 UTC, and (b) days with thunderstorms: at least one ANETZ station has reported at least one near lightning between 1240 and 2340 UTC. In addition, the days with thunderstorms were further stratified into (c) days with isolated thunderstorms: the criterion for ''days with thunderstorms'' is fulfilled, but the criterion for ''days with widespread and severe thunderstorms'' is not fulfilled; and (d) days with widespread and severe thunderstorms: at least 12 ANETZ stations have reported near lightnings between 1240 and 2340 UTC and in addition (as a severity criterion) at least 20 communities have reported hail damage.

The remaining 516 days were thereafter divided into 357 days without thunderstorms (69%) and 159 days with thunderstorms (31%). The days with thunderstorms were once more stratified into 139 days with isolated thunderstorms (87%) and 20 days with widespread and severe thunderstorms (13%).

b. Thermodynamic and kinematic parameters

Only thermodynamic and kinematic parameters, which represent stability and vertical wind shear (the latter influencing the convective strength and organization), were calculated from the radiosondes in Payerne (z_0 = 491 m). The parameters are listed below in this section and an overview (parameter, code, key references, equations, remarks) is given in the appendix. The majority of the stability indices include only the temperature and humidity values at critical standard pressure levels for the calculation of the stability. These indices were developed in order to give the forecaster an indication of how stable or unstable the conditions are that predominate the atmosphere. In contrast to the calculation of these stability indices, the more recently developed CAPE is an integral value of the convective available potential energy throughout most of the troposphere, including more than just values from the critical standard pressure levels. This means that the CAPE parameters presented below are useful for the determination of the convective strength and that the non-CAPE stability indices are more successful by the decision stable or unstable environment (that means if an air mass has any thunderstorm potential at all).

The parameters include 1) wind shear: vertical wind shear of the horizontal wind (surface–3 km, 3–6 km, surface–6 km), and 2) stability indices: K index, TT index, Showalter index (850 hPa), modified Showalter index (700 hPa), modified Showalter index (CCL), modified Showalter index (LCL), surface lifted index, deep convective index, humidity index, Boyden index, KO index, SWEAT index, CAPE (surface), modified CAPE (850 hPa), modified CAPE (CCL), and modified CAPE (LCL).

c. Data analysis

Three methods were used to determine the thermodynamic and kinematic parameters with the strongest relationship to the initiation of thunderstorms in the observation area, namely, 1) skill scores, 2) probability distributions, and 3) mean temperature soundings and hodographs.

1) SKILL SCORES

Skill scores are used in meteorology to verify weather predictions. Thunderstorm predictions have been evaluated with skill scores by, for example, Jacovides and Yonetani (1990), Lee and Passner (1993), and Collier and Lilley (1994). The investigated dataset is divided into a 2 × 2 contingency table with the elements A, B,

		Prediction		
		Event predicted +	Event not predicted -	
Observation	Event observed +	Correct information 40 **A** Correct prediction	No information 10 **B** Surprise	50
	Event not observed -	False information 20 **C** False alarm	Correct information 30 **D** Correct prediction	50
		60	40	100

FIG. 2. Contingency table used to verify predictions (after Hofmann 1974).

C, and D as shown in Fig. 2. The most frequently used skill scores and their codes (CSI, POD, FAR, S, and TSS) are given in Table 1. Each of these elements has certain advantages and disadvantages, and is usually adjusted to particular situations. The disadvantage by applying CSI in comparison with TSS and S is that the correct prediction of the zero events D (Fig. 2) is not considered. Lee and Passner (1993) investigated the occurrence of thunderstorms near 14 sounding stations distributed all over the United States. A thunderstorm event was registered if the thunderstorm occurred within a 100-km area around the station over the 12-h forecast. They found that both skill scores TSS and S give about the same results. The reason is that thunderstorms occur rather frequently near the chosen sounding stations, actually in 34% of the cases. Only in cases of very rare events ($<1\%$) was the skill score S superior, as demonstrated by Doswell et al. (1990). In the present study the most common skill scores like CSI, POD, FAR, S, and TSS were all calculated, but only the TSS values were considered for verification purposes.

2) PROBABILITY DISTRIBUTIONS

Another possibility to determine the most efficient predictand is to plot the probability distributions for a decision variable in different situations (Grosh and Morgan 1975; Mahrt 1977; Modahl 1979; McCoy 1986). In Fig. 3 two relative frequency distributions $f_0(x)$ and $f_1(x)$ are shown as examples for the idealized distribution (Gauss) of the decision variable x on days with and on days without thunderstorms. The value x_G marks the threshold to separate the two probability distributions. In addition, the area below each of the relative frequency distributions corresponds to 100%. The size of the nonoverlapping area corresponds to the efficiency of the predictand. This area is shaded in Fig. 3 for the distribution $f_1(x)$.

3) MEAN TEMPERATURE SOUNDINGS AND HODOGRAPHS

The comparison between mean temperature soundings and mean hodographs on days with and without thunderstorms deepens one's insight into the thermodynamic and kinematic differences of these days. Several methods used to calculate mean temperature soundings and hodographs in the environment of supercells have been summarized by Brown (1993). He used a method that conserves significant features. In a study presented by Bluestein and Jain (1985) several mean temperature soundings and mean hodographs were calculated for different types of squall lines. Similar studies have been carried out by Maddox (1976) and Houze et al. (1990). In contrast to the method used by Brown (1993), a more classic method is used here. Before the mean temperature soundings were calculated, an interpolation at fixed levels was carried out in steps of 250 m except for the first interpolated point (491, 650, 900, 1150, =, 11 900 m). In addition the mean hodographs were also calculated. Hodographs connect the ends of wind vectors in different height levels. Before the mean hodographs were calculated, the wind values (divided into wind components u and v) were also interpolated at fixed levels.

For these calculations, only the months July and August were considered from 1985 to 1989 (310 days). The reason for this restriction is that a mean over all summer months (May–August) contains rather different temperature conditions. In contrast, July and August have about the same temperature and thunderstorm preconditions. For 51 days, no representative sounding was available (see section 3a) and as a result the dataset was reduced to 259 days. This smaller dataset was stratified into 183 days without thunderstorms, 64 days with isolated thunderstorms, and 12 days with widespread and severe thunderstorms—a total of 76 thundery days. The sample seems small. However, the results presented in section 4c are judged to be reliable since similar results were obtained from a preliminary study (not shown here) with a smaller dataset containing only 2 yr (1985 and 1989) instead of 5 yr (1985–89).

4. Results

a. Skill scores

For every thermodynamic and kinematic parameter described in section 3b five skill scores (CSI, POD, FAR, TSS, and S) were derived, but only the values of the TSS were considered to verify the success of the thunderstorm prediction. A guidance value had to be determined for every decision variable to receive the single components A, B, C, and D (Fig. 2). That value

was found at the point where TSS reached a maximum. This optimized guidance value divided the dataset into two groups. One group contained the values larger than the determined value. This means for an index like the K index, which ideally increases with increasing thunderstorm activity, that thunderstorms were predicted as long as the guidance value was exceeded. In contrast, if the values were smaller than the determined value, no thunderstorms were predicted. For an index like the Showalter index, which ideally decreases with increasing thunderstorm activity, the conditions were reversed.

In Table 2 five skill scores for 16 stability indices are shown for the prediction of nonthundery and thundery days, respectively. For the decision at 0000 UTC, whether a thundery day will be expected or not, the use of the original Showalter index (850 hPa) showed the highest TSS skill score. The guidance value for SI_{850} was determined to be 1.8°C (Table 2). In this case thunderstorms were predicted as long as this value was not exceeded. At 1200 UTC the highest TSS skill score for the same prediction was reached by using the SWEAT index with the guidance value >60 (no dimension).

The decision at 0000 UTC, whether a day with isolated or widespread thunderstorms will be expected, was most successful by using the stability indices SI_{LCL} (<−0.5°C) or SLI (<1.4°C), see Table 3. At 1200 UTC the indices DCI (>20.3°C) and $CAPE_{CCL}$ (>500 J kg^{-1}) showed the best results.

In addition to the stability the wind shear belongs to the most important parameters for the prediction of thunderstorms (important for the thunderstorm organization). On days with forthcoming thunderstorm activity, weak wind shear was present at 0000 UTC in the layer between 3 and 6 km (TSS = 0.21). In contrast, strong wind shear was apparent at 1200 UTC in the layer between the surface and 3 km (TSS = 0.26).

b. Probability distributions

In Fig. 4a the probability distribution for the best stability index at 0000 UTC, namely SI_{850} (see Table 2), is shown for nonthundery and thundery days, respectively. The interval of each class is 0.1°C. The probability distributions were slightly smoothed to ignore isolated zero values in frequency. The guidance temperature value, where the two distributions coincide (dashed line), is given in the legend of the figure. Most important is the size of the area that is not jointly covered. For SI_{850} this area reached 30%. In comparison the probability distribution of the KO index is shown in Fig. 4b (the rest of the stability indices are not shown because of the lack of space). It is obvious that the success by using this index was remarkably smaller than for SI_{850}. The area, where the two distributions do not overlap, is only 19%.

The best results were achieved by using the 1200 UTC stability indices instead of the 0000 UTC ones. This result is reasonable, given the temporal proximity of the 1200 UTC sounding to diurnal convection initiation. In Fig. 5a the probability distribution of SI_{850} at noon is shown. In this case the nonoverlapping area increased to 48%. The best stability index at noon UTC (Table 2b) is the SWEAT index. In Fig. 5b the probability distribution of this index is presented. This index shows an even greater nonoverlapping area of 53% in comparison to SI_{850}. No probability distributions were calculated for the categories with isolated and widespread thunderstorm days because of the small number of data.

c. Mean temperature soundings and hodographs

The comparison of the three mean temperature soundings for no, isolated, and widespread thunderstorm days shows a strong correlation between the instability and the forthcoming thunderstorm activity. On average no $CAPE_{CCL}$ (0 J kg^{-1}) was available on days without thunderstorms, neither at 0000 nor as well as at 1200 UTC. Days with isolated thunderstorms showed an average $CAPE_{CCL}$ of 210 J kg^{-1} at 0000 and 400 J kg^{-1} at 1200 UTC. In comparison the days with widespread thunderstorms showed an average $CAPE_{CCL}$ of 1150 J kg^{-1} at 0000 and 1060 J kg^{-1} at 1200 UTC.

The differences in the instability appear more pronounced if the differences between the three mean temperature soundings are determined (Figs. 6a–d). The most significant temperature differences were generally obtained in the layer between 1.5 and 2 km (~850 hPa). In this layer the mean 0000 UTC sounding from the days with isolated thunderstorms was approximately 3°C warmer (Fig. 6a) than for the days without thunderstorms. The same comparison for days with widespread thunderstorms showed an approximately 6°C warmer layer (Fig. 6b). At 1200 UTC this warm layer also appeared at the surface (Fig. 6c). In general the positive temperature difference reduced markedly in the layer between 2 and 5 km (~500 hPa). Above 5 km no large temperature differences were obtained in comparison to the days without thunderstorms. Obviously, on thundery days an especially strong conditionally unstable layer is present between 850 and 500 hPa.

In Figs. 6a–d the differences between the mean dewpoint depression ($T–T_d$) soundings are also presented. The reason for showing the dewpoint depression ($T–T_d$) instead of the dewpoint (T_d) is that the dewpoint depression is well correlated with the relative humidity in a temperature range typical for summertime conditions. The most striking differences between the mean dewpoint depression soundings occur in the layer between 3 and 4 km (600–700 hPa). On thundery days this layer was especially humid (small dewpoint depression) in comparison to the conditions on nonthundery days. This results in an especially strong difference between the two mean dewpoint depression soundings in this layer as shown in Figs. 6a–d. For instance the dewpoint depression was approximately 7°C lower at 1200 UTC on

TABLE 1. Overview of the most frequently used skill scores.

Skill score	Code	Reference(s)	Equation	Limits
Probability of detection	POD	Donaldson et al. (1975)	$\mathrm{POD} = \frac{A}{A + B}$	$0 \le \mathrm{POD} \le 1$
False alarm ratio	FAR	Donaldson et al. (1975)	$\mathrm{FAR} = \frac{C}{A + C}$	$0 \le \mathrm{FAR} \le 1$
Critical success index ("threat score")	CSI	Donaldson et al. (1975)	$\mathrm{CSI} = \frac{A}{A + B + C}$	$0 \le \mathrm{CSI} \le 1$
True skill statistics	TSS	Hanssen and Kuipers (1965) Hofmann (1974) Doswell and Flueck (1989)	$\mathrm{TSS} = \frac{A}{A + B} - \frac{C}{C + D}$	$-1 \le \mathrm{TSS} \le 1$
Heidke skill score	S	Brier and Allen (1952)	$S = \frac{2(AD - BC)}{(A + B)(B + D) + (A + C)(C + D)}$	$-1 \le S \le 1$

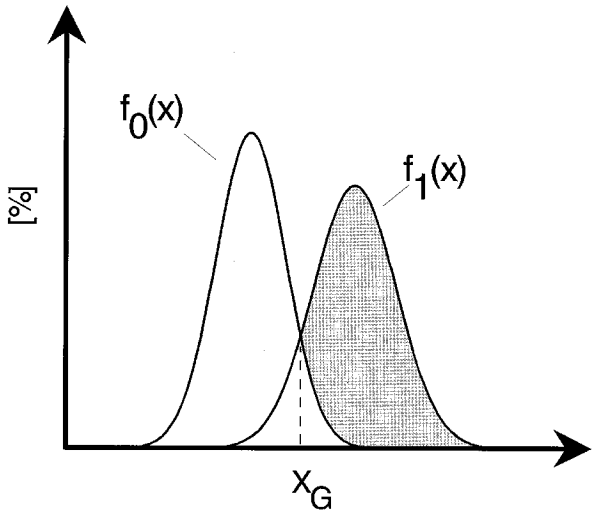

FIG. 3. Probability distributions of the decision variable x indicating the occurrence (f_0)/nonoccurrence (f_1) of a predictand. The value x_G marks the threshold to separate the two probability distributions. The size of the shaded area corresponds to the efficiency of the decision variable x.

thundery days (Figs. 6c and 6d). This reservoir of humid air about 1000 m above the condensation level seems to be very important for the further development of strong thunderstorms.

The comparison of mean hodographs shows marked differences for the three thunderstorm categories (Fig. 7). The distinct low-level jet at 3 km on thundery days is remarkable (Figs. 7b and 7c), and the southwesterly or westerly winds dominated through the whole troposphere. On the contrary, no pronounced low-level jet was present on nonthundery days (Fig. 7a), and the mean wind direction veered to the west or northwest above 3 km. The southwesterly or westerly winds are important for the advection of warm and humid air from the Mediterranean region (Huntrieser et al. 1994a), and the pronounced low-level jet influences the organization of the thunderstorms. The unstable layer between 850 and 500 hPa over northern Switzerland on thundery days develops when warm air in the lower layer is transported from the Mediterranean region by southwesterly winds (mostly in the warm sector of a low) and colder air is advected in higher levels from the approaching trough from the west.

For a more detailed investigation of the differences between the hodographs, the wind vectors were divided into their components u and v. The v component (north–south) is the most important component for the initiation of thunderstorms. On forthcoming thundery days a strongly increasing southerly wind component was observed through the lowest 3 km (Fig. 8). In the layer above (3–6 km) the influence of the southern component decreased clearly. However, in the upper troposphere the southern component increased again. The mean vertical wind profiles showed very similar conditions on

TABLE 2. Comparison of five skill scores for 16 stability indices used for the prediction nonthundery/thundery days at (a) 0000 UTC and (b) 1200 UTC. Bold values indicate the 5 stability indices with the highest skill scores.

Stability index	Limit	CSI	POD	FAR	S	TSS
(a) 0000 UTC						
K	>24	0.385	0.745	0.557	**0.276**	**0.328**
TT	>45	0.352	0.745	0.599	0.200	0.248
SI_{850}	<1.8	0.381	0.561	0.457	**0.347**	**0.350**
SI_{700}	<4.1	0.387	0.711	0.540	0.266	**0.303**
SI_{CCL}	<1.0	0.379	0.815	0.586	0.237	0.301
SI_{LCL}	<1.2	0.362	0.541	0.479	**0.316**	**0.320**
SLI	<5.1	0.349	0.752	0.605	0.190	0.237
DCI	>14.9	0.348	0.561	0.522	**0.275**	0.288
HI	<25.1	0.306	0.694	0.646	0.102	0.129
BI	>51.4	0.371	0.828	0.598	0.216	0.280
KO	<0.3	0.322	0.605	0.592	0.188	0.213
SWEAT	>83	0.377	0.745	0.567	0.259	**0.311**
$CAPE_{Surface}$	>50	0.160	0.204	0.573	0.095	0.082
$CAPE_{850}$	>15	0.300	0.439	0.514	0.238	0.232
$CAPE_{CCL}$	>300	0.343	0.510	0.487	**0.294**	0.294
$CAPE_{LCL}$	>20	0.309	0.510	0.560	0.210	0.220
(b) 1200 UTC						
K	>22	0.482	0.830	0.466	**0.440**	**0.508**
TT	>46	0.483	0.704	0.395	**0.478**	**0.500**
SI_{850}	<3.9	0.473	0.780	0.454	**0.439**	**0.491**
SI_{700}	<5.6	0.444	0.868	0.524	0.360	0.442
SI_{CCL}	<0.2	0.380	0.711	0.550	0.279	0.324
SI_{LCL}	<1.4	0.477	0.717	0.412	**0.465**	**0.493**
SLI	<0.7	0.464	0.843	0.492	0.405	0.479
DCI	>18.4	0.393	0.579	0.449	0.363	0.369
HI	<32.0	0.358	0.811	0.609	0.191	0.248
BI	>51.9	0.439	0.811	0.511	0.366	0.433
KO	<−3.5	0.395	0.673	0.511	0.325	0.359
SWEAT	>60	0.515	0.780	0.398	**0.507**	**0.548**
$CAPE_{Surface}$	>200	0.461	0.711	0.432	0.439	0.470
$CAPE_{850}$	>0	0.356	0.484	0.425	0.339	0.325
$CAPE_{CCL}$	>70	0.388	0.734	0.549	0.289	0.339
$CAPE_{LCL}$	>40	0.418	0.642	0.455	0.385	0.403

TABLE 3. Comparison of five skill scores for 16 stability indices used for the prediction isolated/widespread thunderstorms at (a) 0000 UTC and (b) 1200 UTC. Bold values indicate the 5 stability indices with the highest skill scores.

Stability index	Limit	CSI	POD	FAR	S	TSS
(a) 0000 UTC						
K	>29	0.197	0.750	0.789	0.166	0.347
TT	>48	0.190	0.800	0.800	0.149	0.340
SI_{850}	<0.1	0.283	0.650	0.667	**0.329**	**0.463**
SI_{700}	<1.0	0.250	0.421	0.619	**0.310**	0.324
SI_{CCL}	<−2.1	0.250	0.750	0.727	0.264	0.462
SI_{LCL}	<−0.5	0.333	0.700	0.611	**0.404**	**0.542**
SLI	<1.4	0.271	0.800	0.709	0.297	**0.519**
DCI	>17.3	0.250	0.850	0.738	0.257	**0.505**
HI	>23.0	0.167	0.550	0.807	0.122	0.219
BI	>53.1	0.209	0.450	0.719	0.226	0.285
KO	<−3.5	0.283	0.650	0.667	**0.329**	0.463
SWEAT	>219	0.256	0.500	0.655	0.305	0.363
$CAPE_{Surface}$	>30	0.262	0.550	0.667	0.305	0.389
$CAPE_{850}$	>70	0.273	0.600	0.667	**0.318**	0.427
$CAPE_{CCL}$	>650	0.263	0.750	0.712	0.285	**0.480**
$CAPE_{LCL}$	>100	0.241	0.650	0.723	0.257	0.405
(b) 1200 UTC						
K	>29	0.155	0.450	0.809	0.110	0.173
TT	>51	0.182	0.400	0.750	0.179	0.225
SI_{850}	<−1.5	0.273	0.300	0.250	**0.384**	0.285
SI_{700}	<3.1	0.171	0.650	0.812	0.118	0.241
SI_{CCL}	<−2.1	0.273	0.750	0.700	0.301	**0.495**
SI_{LCL}	<−1.3	0.250	0.650	0.711	0.272	0.416
SLI	<−3.5	0.304	0.700	0.650	**0.358**	**0.510**
DCI	>20.3	0.253	0.950	0.743	0.255	**0.549**
HI	>22.5	0.189	0.700	0.794	0.151	0.306
BI	>53.3	0.160	0.400	0.789	0.131	0.181
KO	<−7.4	0.268	0.750	0.706	0.293	0.487
SWEAT	>230	0.241	0.350	0.562	**0.311**	0.284
$CAPE_{Surface}$	>1400	0.343	0.600	0.556	**0.427**	**0.491**
$CAPE_{850}$	>100	0.176	0.300	0.700	0.198	0.198
$CAPE_{CCL}$	>500	0.276	0.800	0.704	**0.303**	**0.523**
$CAPE_{LCL}$	>300	0.255	0.650	0.705	0.280	0.424

days with isolated and widespread thunderstorms. On the contrary, the days without thunderstorm activity showed that the northern component was more dominating. A light southerly component was visible only in the layer between 2 and 3 km.

The second wind component *u* (east–west) showed no such striking differences as obtained for the *v* component. However, on thundery days an especially strong increase of westerly winds in the lowest layer (surface–3 km) was also observed for this component. In the midlayer (3–6 km) the increase with height was minor. In contrast the days without thunderstorms showed a regular increasing westerly wind component through the lowest 6 km.

The above-mentioned differences indicate which levels (for temperature, relative humidity, and wind shear) correlate best with the development of thunderstorms in Switzerland. The same levels are also used for the calculation of the indices with the best results (see section 4a and the appendix) as the original Showalter index (includes T_{850} and T_{500}), the SWEAT index (contains T_{850}–T_{500} and wind shear between 850 and 500 hPa), and the K index (contains T_{850}– T_{500} and T_{700}–Td_{700}).

d. Discussion of the results

The results of our study have shown that stability indices are important thunderstorm predictors. The best index to use at 0000 UTC for the prediction of a nonthundery or thundery day is the original Showalter index (SI_{850}). At 1200 UTC the best results are obtained with the combined SWEAT index closely followed by the original Showalter index (SI_{850}). The $CAPE_{CCL}$ and DCI belong to the most successful parameters whether isolated or widespread thunderstorms are expected.

Besides the stability indices, the vertical wind shear and the relative humidity show a marked correlation to the development of thunderstorms. On days with forthcoming thunderstorm activity the wind shear in the layer between 3 and 6 km is weak at 0000 UTC. On the contrary, strong wind shear between the surface and 3 km (low-level jet) is present at 1200 UTC. The analysis

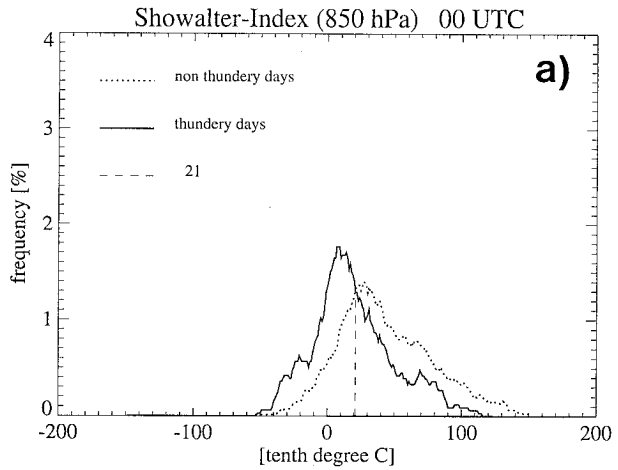

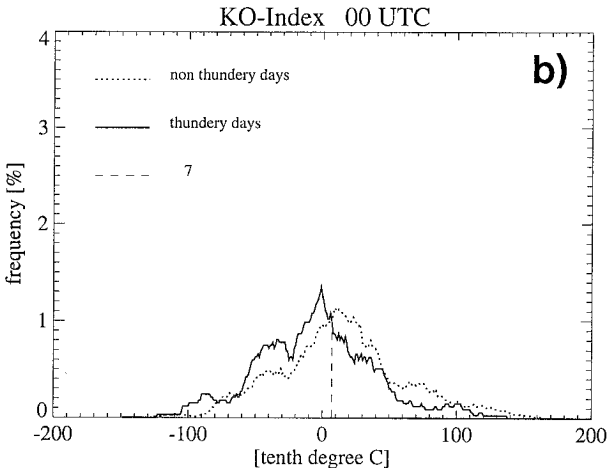

FIG. 4. The relative frequency distribution of (a) the original Showalter index and (b) the KO index at 0000 UTC.

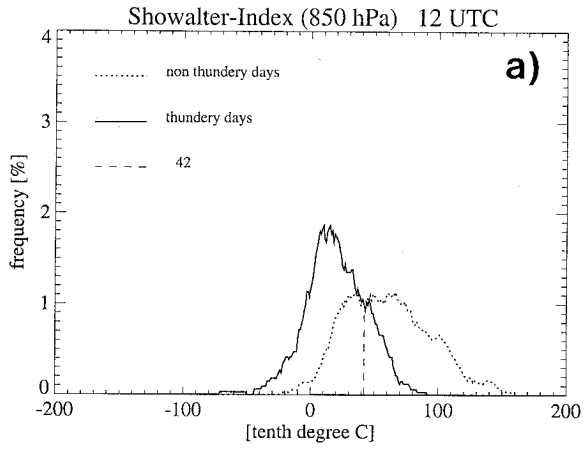

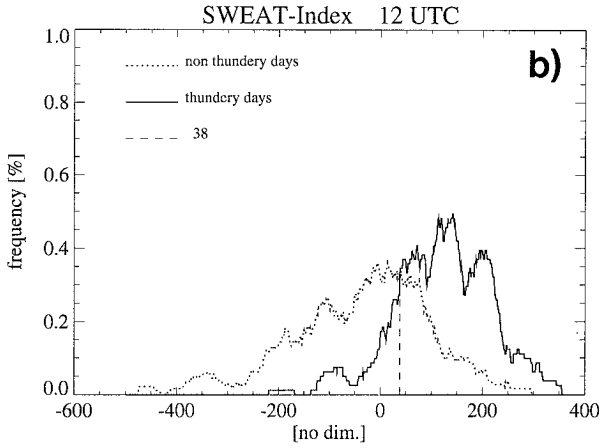

FIG. 5. The relative frequency distribution of (a) the original Showalter index and (b) the SWEAT index at 1200 UTC.

of the relative humidity (dewpoint depression used) revealed for thundery days a drier layer in 850 hPa at 0000 UTC and a more humid layer in 700 hPa at 1200 UTC than for nonthundery days.

The results of the present study show several similarities to the ones from Florida published recently by Fuelberg and Biggar (1994), who received the best results with the stability index SLI. As a whole, their results were not as good as those presented for Switzerland. For instance, the separation of mean values, skill scores, and probability distributions for the different thunderstorm categories no convection/weak convection/strong convection was less successful as in the present study. Fuelberg and Biggar obtained the following mean values and standard deviations for SLI [°C]: strong convection, -6.5 ± 1.8; weak convection, -5.2 ± 2.1; and no convection, -3.7 ± 3.0. For Switzerland the corresponding values are widespread and severe: thunderstorms, -4.1 ± 2.6; isolated thunderstorms, -1.6 ± 2.5; and no thunderstorms, 2.2 ± 3.5. The reasons for the better results in Switzerland are unknown. Perhaps the different definition of the thunderstorm days has an influence, or the better results were achieved because of the larger dataset. Fuelberg and Biggar (1994) also found large differences in the wind direction on days with and without convection. In Florida, strong convection was always coupled with southwesterly winds. In contrast, the north to northwesterly winds were dominant on days with no convection. A humid layer between 700 and 500 hPa was also observed.

The mean vertical wind profiles (u and v components), as described in section 4c for Switzerland, show similarities to the profiles presented by Brown (1993, Fig. 4) for days with supercell thunderstorms in the United States. The only striking difference is the height of the low-level jet. In Switzerland the maximum of this jet is observed at 3 km (~700 hPa), probably influenced by the Alps. In comparison Brown (1993) detected this

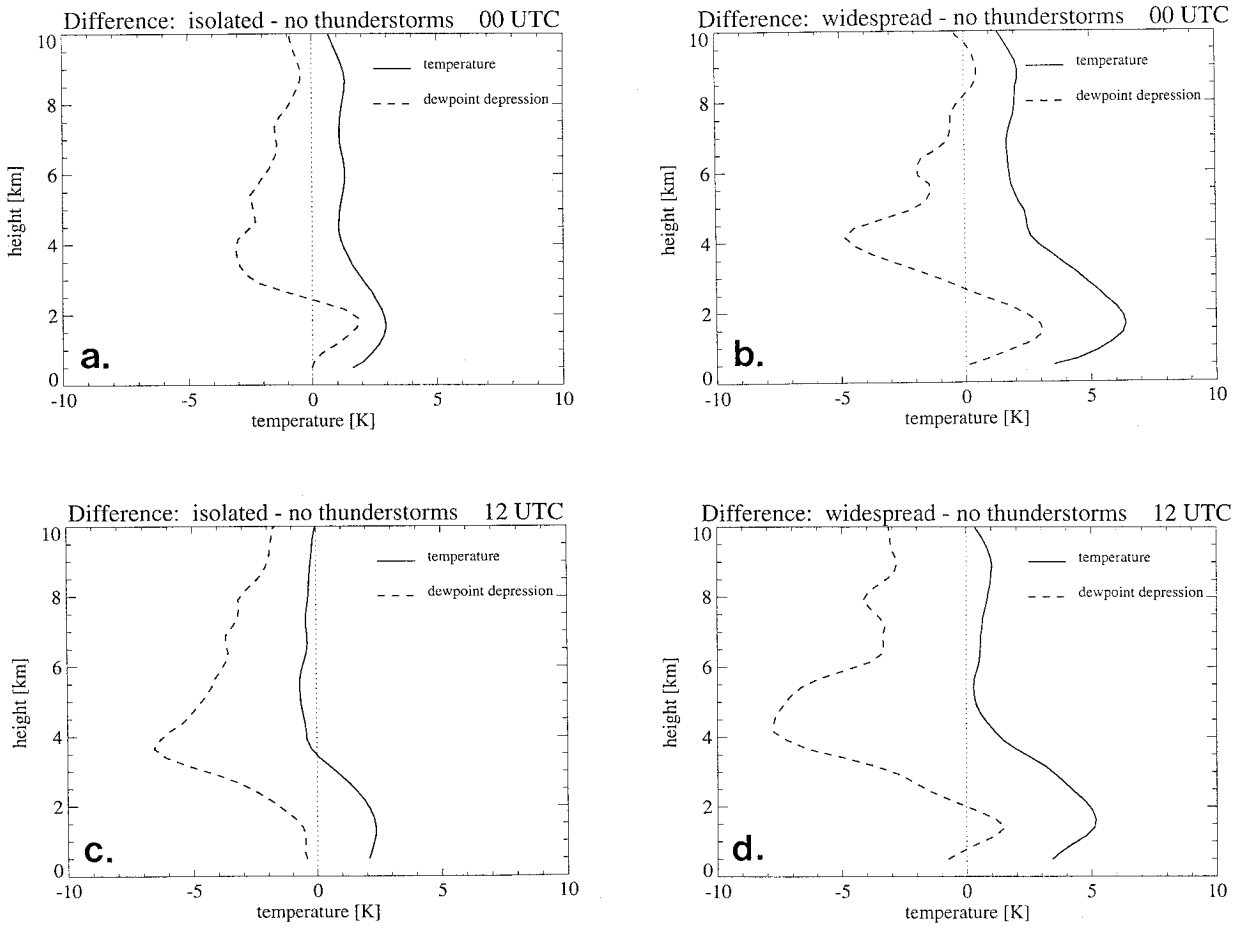

FIG. 6. Difference between the mean temperature soundings (temperature and dewpoint depression) (a) on days with isolated thunderstorms and days without thunderstorms at 0000 UTC (b) on days with widespread thunderstorms and days without thunderstorms at 0000 UTC, (c) on days with isolated thunderstorms and days without thunderstorms at 1200 UTC and (d) on days with widespread thunderstorms and days without thunderstorms at 1200 UTC.

jet maximum at 1.5-km height (~850 hPa) for the United States (see also Houze et al. 1993; Maddox 1976).

5. New thunderstorm indices

a. Development of the indices

The thermodynamic and kinematic parameters with the strongest relationship to the thunderstorm initiation such as stability, wind shear, and relative humidity (section 4) are combined to create new thunderstorm indices specially adjusted to the conditions in northern Switzerland. This method is similar to the calculations of the well-known SWEAT index in the United States. The thunderstorm indices designed for Switzerland are called $SWISS_{00}$ index (calculated from the 0000 UTC sounding in Payerne) and $SWISS_{12}$ index (1200 UTC sounding). The two SWISS indices can be used as relatively reliable guidance for forecasting thunderstorms in the northern part of Switzerland. The $SWISS_{00}$ index contains the most important thunderstorm parameters at 0000 UTC as the original Showalter index (SI_{850}), the wind shear (WSh) between 3 and 6 km, and the dewpoint depression ($T - T_d$) at 600 hPa. All of these parameters are particularly small on days with thunderstorms. Various tests (including regression analysis) have resulted in the following linear combination with the highest TSS value calculated from the midnight sounding (Huntrieser 1995):

$$SWISS_{00} = SI_{850} + \frac{4}{10}WSh_{3-6} + \frac{1}{10}(T - T_d)_{600}$$

$$[°C][m\,s^{-1}(3\,km)^{-1}][°C]. \quad (1)$$

The guidance value for the occurrence of thunderstorms was determined to be <5.1 (no dimension). In the contingency table presented in Table 4 the thunderstorm prediction under the application of the new $SWISS_{00}$ index part b was compared to the results by applying the original Showalter index part a. The new $SWISS_{00}$ index (TSS = 0.374) barely showed better results in comparison to the original Showalter index (TSS = 0.350). The application of the new $SWISS_{00}$

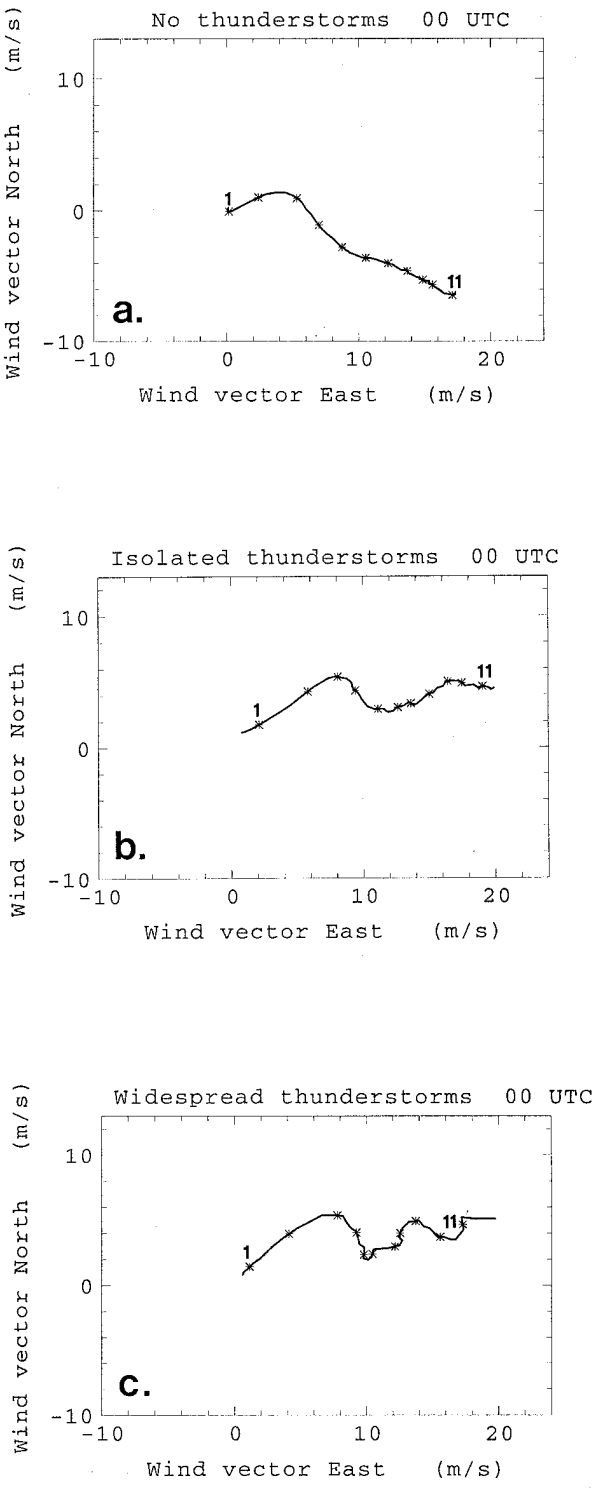

FIG. 7. Comparison between the mean 0000 UTC hodographs for no/isolated/widespread thunderstorm days (first * = 1 km, last * = 11 km).

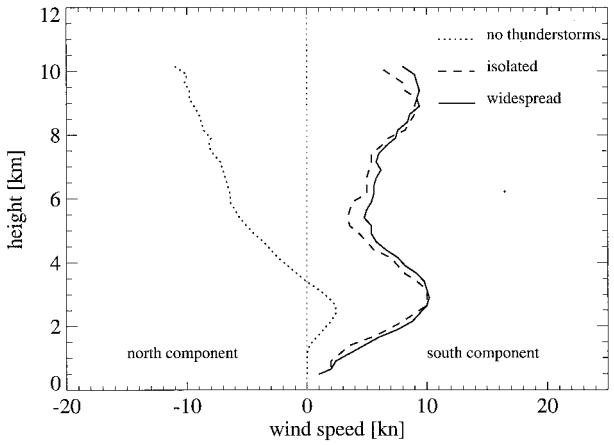

FIG. 8. Comparison between the mean 0000 UTC vertical windprofiles (v component) for no/isolated/widespread thunderstorm days.

index resulted in 73% correctly predicted cases, 13% missed cases, and 14% cases with false alarms (Table 4b).

However, the thunderstorm prediction can be improved at 0000 UTC if the current synoptic situation is considered. Thunderstorms can also be expected under certain circumstances if the $SWISS_{00}$ index or the original Showalter index exceed the guidance value. The requirement is that a cold front is expected to pass through Switzerland during the second half of the day (1200–2400 UTC). In addition, the weather situation (geostrophic wind direction) is not allowed to include a northern wind component. These days are characterized by a strong diurnal change in stability caused by the approach of a cold front (advection of warm and cold air in different heights). The additional synoptic criteria improved the correct prediction by applying the $SWISS_{00}$ index by about 3% as shown in Table 4d. The TSS value increased from 0.374 to 0.501, which means

TABLE 4. Verification of thunderstorm predictions under application of (a) the original Showalter index, (b) the new $SWISS_{00}$ index, (c) the original Showalter index combined with synoptic information, and (d) the new $SWISS_{00}$ index combined with synoptic information at 0000 UTC.

0000 UTC

		Prediction	
Stability index	Observation	Thundery day (%)	Nonthundery day (%)
(a) SI_{850}	Thundery day	17	13
	Nonthundery day	15	55
(b) $SWISS_{00}$	Thundery day	18	13
	Nonthundery day	14	55
(c) SI_{850} + synoptic	Thundery day	22	9
	Nonthundery day	17	52
(d) $SWISS_{00}$ + synoptic	Thundery day	23	8
	Nonthundery day	16	53

TABLE 5. Verification of thunderstorm predictions under application of (a) the surface lifted index, (b) the SWEAT index, and (c) the new $SWISS_{12}$ index at 1200 UTC.

1200 UTC

Stability index	Observation	Prediction: Thundery day (%)	Prediction: Non-thundery day (%)
(a) SLI	Thundery day	26	5
	Nonthundery day	25	44
(b) SWEAT	Thundery day	24	7
	Nonthundery day	16	53
(c) $SWISS_{12}$	Thundery day	26	5
	Nonthundery day	17	52

TABLE 6. Verification of thunderstorm predictions under application of (a) the $CAPE_{CCL}$ and (b) the deep convective index at 0000 UTC.

0000 UTC

Stability index	Observation	Prediction: Widespread (%)	Prediction: Isolated (%)
(a) $CAPE_{CCL}$	Widespread	10	3
	Isolated	23	64
(b) DCI	Widespread	11	2
	Isolated	30	57

76% of the cases are correctly predicted, 8% are missed cases, and 16% are false alarm cases. The reduction of the missed cases from 13% to 8% by adding the synoptic situation to the $SWISS_{00}$ index is remarkable. By applying the original Showalter index combined with the synoptic situation, the TSS value increased from 0.350 to 0.480, which means 74% of the cases are correctly predicted, 9% are missed cases, and 17% are false alarm cases (Table 4c). The improvement by using the synoptic criteria to the $SWISS_{00}$ index is more successful than the one of the original Showalter index.

At 1200 UTC, the SLI combined with WSh between the surface and 3 km and the dewpoint depression ($T - T_d$) at 650 hPa shows the best results ($SWISS_{12}$ index) for the decision of whether a thunderstorm day is expected or not. The wind shear is particularly large on days with forthcoming thunderstorms. In contrast, the other two parameters are particularly small. The following linear combination was calculated from the 1200 UTC sounding with the highest TSS value:

$$SWISS_{12} = SLI - \frac{3}{10}WSH_{0-3} + \frac{3}{10}(T - T_d)_{650}$$

$$[°C] \quad [m\ s^{-1}(3\ km)^{-1}][°C]. \qquad (2)$$

The guidance value for the occurrence of thunderstorms was determined to be <0.6 (no dimension). In Table 5 the new $SWISS_{12}$ index is compared to the SWEAT index and the surface lifted index. The results show that the application of the new $SWISS_{12}$ index (TSS = 0.587) is better than the SWEAT index (TSS = 0.548) but significantly better than the SLI (TSS = 0.479) alone. Under the application of the $SWISS_{12}$ index, 78% of the cases are correctly predicted, only 5% are missed cases, and 17% are false alarm cases (Table 5c). This is an even better result than that obtained at 0000 UTC (Table 4). The low number of missed cases is especially striking. No improvement of the $SWISS_{12}$ index was reached by considering the present synoptic situation (especially cold front passages). The $SWISS_{12}$ index is probably a better indicator for the diurnal preconvective situation than a 0000 UTC index.

The probability distributions were calculated for the SWISS indices, confirming the results from the skill score TSS, which show that the new SWISS indices reached the highest scores. For the $SWISS_{00}$ index the nonoverlapping area of the two distributions on thundery and nonthundery days increases to 35% (original Showalter index 30%). The $SWISS_{12}$ index shows similar improvements. The nonoverlapping area increases from 53% (SWEAT index) to 57% ($SWISS_{12}$ index).

For the decision, between an isolated and widespread thunderstorm day, no suitable combined thunderstorm index was found at 0000 UTC, probably because of the small dataset. Instead it is suggested to use the $CAPE_{CCL}$ only (TSS = 0.480) with the guidance value >650 J kg^{-1} for widespread thunderstorms or the DCI (TSS = 0.505) with the guidance value >17.3°C. The verification of these two indices is presented in Table 6. A correct prediction with the application of $CAPE_{CCL}$ is reached in 74% of the cases, only 3% are missed, and 23% are false alarm cases.

At 1200 UTC the best index for the decision between isolated and widespread thunderstorm days is a combination of $CAPE_{CCL}$ and the wind shear S in the lowest 6 km. This wind shear S is the same as used for the calculations of the bulk Richarson number (see the appendix). Both S and $CAPE_{CCL}$ have especially high values on days with widespread thunderstorms. This third new combined thunderstorm index is called the CS index:

$$CS = CAPE_{CCL}S$$

$$[J\ kg^{-1}][m\ s^{-1}(6\ km)^{-1}]. \qquad (3)$$

The CS index (TSS = 0.515) is similar to the energy–helicity index presented by Hart and Korotky (1991). The guidance value of the CS index exceeded > 2700 [J kg^{-1} m s^{-1} (6 km)$^{-1}$] for the prediction of widespread thunderstorms. The contingency table (not presented here) showed that the application of the CS index resulted in 72% correct predictions, 3% missed cases, and 25% false alarm cases.

b. Verification of the indices

The next step is to examine how useful these indices are in comparison to the traditional indices presented in

TABLE 7. Comparison of five skill scores for 16 traditional stability indices and the newly developed SWISS index (test dataset) used for the prediction nonthundery/thundery days at (a) 0000 UTC and (b) 1200 UTC. Bold values indicate the 5 stability indices with the highest skill scores.

Stability index	Limit	CSI	POD	FAR	S	TSS
(a) 0000 UTC						
K	>24	0.350	0.683	0.582	0.172	0.198
TT	>45	0.434	0.851	0.530	**0.302**	**0.362**
SI_{850}	<1.8	0.388	0.584	0.464	**0.320**	**0.327**
SI_{700}	<4.1	0.369	0.644	0.536	0.242	0.265
SI_{CCL}	<1.0	0.420	0.881	0.555	0.259	0.321
SI_{LCL}	<1.2	0.416	0.634	0.453	**0.352**	**0.366**
SLI	<5.1	0.415	0.842	0.550	0.261	0.316
DCI	>14.9	0.364	0.584	0.508	0.264	0.276
HI	<25.1	0.241	0.485	0.675	−0.027	−0.030
BI	>51.4	0.362	0.762	0.593	0.160	0.194
KO	<0.3	0.447	0.832	0.509	**0.335**	**0.392**
SWEAT	>83	0.409	0.733	0.519	**0.290**	**0.327**
$CAPE_{Surface}$	>50	0.143	0.178	0.581	0.060	0.051
$CAPE_{850}$	>15	0.270	0.366	0.493	0.197	0.184
$CAPE_{CCL}$	>300	0.342	0.535	0.514	0.241	0.247
$CAPE_{LCL}$	>20	0.335	0.545	0.534	0.217	0.226
$Swiss_{00}$	<5.1	0.444	0.663	0.427	**0.395**	**0.411**
(b) 1200 UTC						
K	>22	0.357	0.495	0.438	0.307	0.298
TT	>46	0.424	0.525	0.312	**0.428**	0.404
SI_{850}	<3.9	0.515	0.693	0.333	**0.511**	**0.516**
SI_{700}	<5.6	0.448	0.733	0.464	0.376	**0.409**
SI_{CCL}	<0.2	0.367	0.683	0.558	0.215	0.244
SI_{LCL}	<1.4	0.467	0.634	0.360	**0.453**	**0.452**
SLI	<0.7	0.500	0.891	0.467	**0.422**	**0.492**
DCI	>18.4	0.356	0.525	0.475	0.282	0.282
HI	<32.0	0.299	0.495	0.569	0.156	0.162
BI	>51.9	0.426	0.683	0.469	0.350	0.375
KO	<−3.5	0.397	0.683	0.514	0.286	0.314
SWEAT	>60	0.416	0.515	0.316	**0.417**	0.392
$CAPE_{Surface}$	>200	0.465	0.730	0.438	0.412	**0.442**
$CAPE_{850}$	>0	0.202	0.218	0.267	0.214	0.177
$CAPE_{CCL}$	>70	0.376	0.693	0.548	0.233	0.264
$CAPE_{LCL}$	>40	0.406	0.515	0.342	0.400	0.378
$Swiss_{12}$	<0.6	0.542	0.762	0.347	**0.533**	**0.555**

the appendix. For this verification an independent dataset is used [''cross validation''; Mosteller and Tukey (1977)] including the summer months from May to August 1990, 1992, and 1993 (no data were available for 1991). The original dataset contains 369 days, whereby on 70 days no representative or complete soundings are available (section 3a). The remaining days are divided into 198 days without thunderstorms and 101 days with thunderstorms. The thunderstorm days are further divided into 82 days with isolated thunderstorms and 19 days with widespread and severe thunderstorms. The same calculations as presented in section 3c are carried out.

The most useful stability indices at 0000 UTC for the prediction of days with or without thunderstorms by considering the TSS skill score are (see Table 7a) KO (0.392), SI_{LCL} (0.366), TT (0.362), SI_{850} (0.327), and SWEAT (0.327). In comparison the $SWISS_{00}$ index shows the best result with TSS = 0.411. The guidance values derived from the original dataset (May–August 1985–89) were used. Table 8 shows the improvements for the test dataset by using $SWISS_{00}$ index combined with the synoptic situation (TSS = 0.543) instead of the best traditional index (SI_{850}). The percentage of missed forecasts decreases from 14% to 5%, and the ratio of the correct predictions increases from 69% to 75%. In comparison the improvements by using the original Showalter index (SI_{850}) combined with the synoptic situation (TSS = 0.381) are not that successful: the percentage of missed forecasts decreases from 14% to 11%, and the ratio of the correct predictions increases from 69% to 70%.

TABLE 8. Verification of thunderstorm predictions under application of (a) the original Showalter index, (b) the new $SWISS_{00}$ index, (c) the original Showalter index combined with synoptic information, and (d) the new $SWISS_{00}$ index combined with synoptic information at 0000 UTC for the test dataset.

0000 UTC		Prediction	
Stability index	Observation	Thundery day (%)	Nonthundery day (%)
(a) SI_{850}	Thundery day	20	14
	Nonthundery day	17	49
(b) $SWISS_{00}$	Thundery day	23	11
	Nonthundery day	17	49
(c) SI_{850} + synoptic	Thundery day	22	11
	Nonthundery day	19	48
(d) $SWISS_{00}$ + synoptic	Thundery day	29	5
	Nonthundery day	20	46

At 1200 UTC the best results for the traditional indices are obtained for SI_{850} (TSS = 0.516), SLI (0.492), and SI_{LCL} (0.452), numbers given in Table 7b. Again, the new $SWISS_{12}$ index delivers the best results (TSS = 0.555) from all compared indices. From the numbers in Table 9 the improvements by using the new $SWISS_{12}$ index instead of the SWEAT index (best index 1985–89) or SI_{850} (best index 1990–93) can be clearly seen.

TABLE 9. Verification of thunderstorm predictions under application of (a) the SWEAT index, (b) the original Showalter index, and (c) the new $SWISS_{12}$ index at 1200 UTC for the test dataset.

1200 UTC		Prediction	
Stability index	Observation	Thundery day (%)	Nonthundery day (%)
(a) SWEAT	Thundery day	18	16
	Nonthundery day	8	58
(b) SI_{850}	Thundery day	23	10
	Nonthundery day	12	55
(c) $SWISS_{12}$	Thundery day	26	8
	Nonthundery day	14	52

TABLE 10. Verification of thunderstorm predictions under application of (a) the $CAPE_{CCL}$ and (b) the CS index at 1200 UTC for the test dataset.

1200 UTC			
		Prediction	
Stability index	Observation	Widespread (%)	Isolated (%)
(a) $CAPE_{CCL}$	Widespread	10	9
	Isolated	15	66
(b) CS	Widespread	12	7
	Isolated	14	67

The ratio of the missed cases decreases from 16% to 8%, and the ratio of the correct predictions increases from 76% to 78% by using the new $SWISS_{12}$ index instead of the SWEAT index.

In addition to the TSS skill score, the calculation of the probability distributions shows the best results for the new combined indices. At 0000 UTC the nonoverlapping area of one distribution reaches 42% by using the $SWISS_{00}$ index (here without synoptic). At 1200 UTC the same area for the $SWISS_{12}$ index reaches 56%. The nonoverlapping area is on average ~5% greater than the one of the best traditional index.

As mentioned in section 5a the best thunderstorm index at 0000 UTC for the distinction of isolated or widespread thunderstorm days is the $CAPE_{CCL}$. The verification shows that 70% of the cases are correctly predicted, 9% are missed, and 21% are false alarm cases (TSS = 0.270). For the same prediction at 1200 UTC the best results are obtained with the new combined CS index (TSS = 0.461) in comparison to the best classic index $CAPE_{CCL}$ (TSS = 0.343). The correct prediction increases from 76% to 79%, and the missed cases decrease from 9% to 7% (Table 10).

This verification on an independent test dataset confirms that the new indices give the best results for the thunderstorm prediction. In Table 11 the most important indices and their guidance values are summarized for different thunderstorm classes and times as well as the improvement (in percent) compared to the best traditional index.

6. Summary and conclusions

The prediction of thunderstorms (if, where, and when thunderstorms will occur) is one of the most difficult tasks for a weather forecaster. This paper presents some suggestions on how the thunderstorm prediction in Switzerland north of the Alps can be improved with rather simple methods.

The best traditional index to be used at 0000 UTC for the forecast of a nonthundery or a thundery day is the original Showalter index (SI_{850}) and at 1200 UTC it is the SWEAT index. The $CAPE_{CCL}$ is the most successful parameter at midnight as well as at 1200 UTC for the decision, whether isolated or widespread thunderstorms are expected. The comparison of the mean temperature soundings and hodographs from Payerne for the three thunderstorm categories (no/isolated/widespread) show that the strength of the wind shear and the amount of relative humidity also correlate well with the occurrence of thunderstorms.

The most important parameters like stability, wind shear, and relative humidity are combined in new thunderstorm indices specially adjusted to the conditions in northern Switzerland called SWISS indices. SWISS stands for combined stability and wind shear index for thunderstorms in Switzerland. The SWISS indices are used for the decision of whether a thunderstorm day is to be expected or not. The $SWISS_{00}$ index (calculated from the 0000 UTC radiosounding) contains the original Showalter index, the wind shear between 3 and 6 km, and the dewpoint depression at 600 hPa. All of these parameters are smallest on days with thunderstorms. The thunderstorm prediction can be improved if the current synoptic situation (cold front passage) is considered. At 1200 UTC, the surface lifted index combined with the wind shear between the surface and 3 km and the dewpoint depression at 650 hPa shows the best results ($SWISS_{12}$ index). The wind shear is particularly large

TABLE 11. The most successful Swiss thunderstorm indices and the improvements in comparison to the best traditional indices for the test dataset.

Time (UTC)	Thunderstorm prediction	Best index	Equation	Threshold	Improvement (%) correct cases	Improvement (%) missed cases
0000	Without/with	$SWISS_{00}$	1	<5.1* (no dim.)	+5	−6
1200	Without/with	$SWISS_{12}$	2	<0.6 (no dim.)	+2	−8
0000	Isolated/widespread	$CAPE_{CCL}$	See the appendix	>650 ($J\ kg^{-1}$)	0	0
1200	Isolated/widespread	CS	3	>2700 [$J\ kg^{-1}\ m\ s^{-1}$ $(6\ km)^{-1}$]	+3	−2

* Thunderstorms can also be predicted if $SWISS_{00} \geq 5.1$. The requirements are that a cold front passage is expected over Switzerland during the second half of the day (1200–2400 UTC) and in addition the weather situation (geostrophic wind direction) is not allowed to include a northern wind component.

on days with thunderstorms (low-level jet). In contrast, the other two parameters are particularly small. For the decision of whether a day with isolated or widespread thunderstorms is expected, the best parameter is a combination of $CAPE_{CCL}$ and the wind shear in the lowest 6 km. This new parameter is called the ''CS index.''

All of the traditional and newly created indices used for the thunderstorm prediction were verified on an independent dataset containing 3 yr. The results are satisfactory. The new indices especially designed for northern Switzerland are the best for the prediction of no, isolated, or widespread thunderstorms.

The next step in predicting thunderstorms is to decide more exactly where and when thunderstorms will actually occur. A first attempt in this direction was presented by Huntrieser (1995). In this study a method was developed for the estimation of the regional stability in Switzerland. Temperature and dewpoint values from the ANETZ stations below 1000 m and the temperature value at 500 hPa from the sounding in Payerne were used to calculate the surface lifted index. The spatial distribution of this index was drawn. It became apparent that these fields were not easy to interpret. In addition to stability, the topography plays a crucial role for the initiation of thunderstorms in a mountainous country like Switzerland. Furthermore, the depth of the moist layer, convergence, and the vertical wind shear control the initiation of thunderstorms. Unfortunately, it is not possible at present to determine these quantities on a regional scale. In the future, it is planned to consider the new SWISS index for operational thunderstorm forecasting and for studies in mesoscale numerical prediction models.

Acknowledgments. The authors are grateful to Prof. R. Steinacker from the Institute of Meteorology and Geophysics (University Vienna) for allowing duplication of the orographical map of the alpine region, as presented in Fig. 1, and to W. Henrich from the Institute of Atmospheric Science (ETH Zürich) for modifying this map as desired. Many thanks also to the data providers: Swiss Meteorological Institute and the Swiss Hail Insurance Company. We would like to thank Frank Mair for a thorough and careful reading of the manuscript.

APPENDIX

Summary of Parameters

(See page 124.)

REFERENCES

Andersson, T., M. Andersson, C. Jacobsson, and S. Nilsson, 1989: Thermodynamic indices for forecasting thunderstorms in southern Sweden. *Meteor. Mag.,* **116,** 141–146.

Anthes, R. A., 1976: Numerical prediction of severe storms—Certainty, possibility, or dream? *Bull. Amer. Meteor. Soc.,* **57,** 423–435.

Barlow, W. R., 1993: A new index for the prediction of deep convection. Preprints, *17th Conf. on Severe Local Storms,* St. Louis, MO, Amer. Meteor. Soc., 129–132.

Bidner, A., 1970: The Air Force Global Weather Central severe weather threat (SWEAT) index—A preliminary report. Air Weather Service Aerospace Sciences Review, AWS RP 105-2, No. 70-3, 2-5. [Available from Headquarters, AWS, Scott AFB, IL 62225.]

Bluestein, H. B., and M. H. Jain, 1985: Formation of mesoscale lines of precipitation: Severe squall lines in Oklahoma during the spring. *J. Atmos. Sci.,* **42,** 1711–1732.

Bolton, D., 1980: The computation of equivalent potential temperature. *Mon. Wea. Rev.,* **108,** 1046–1053.

Boyden, C. J., 1963: A simple instability index for use as a synoptic parameter. *Meteor. Mag.,* **92,** 198–210.

Brier, G. W., and R. A. Allen, 1952: Verification of weather forecasts. *Compendium of Meteorology,* Amer. Meteor. Soc., 841–848.

Brown, R. A., 1993: A compositing approach for preserving significant features in atmospheric profiles. *Mon. Wea. Rev.,* **121,** 874–880.

Collier, C. G., and R. B. E. Lilley, 1994: Forecasting thunderstorm initiation in north-west Europe using thermodynamic indices, satellite and radar data. *Meteor. Apps.,* **1,** 74–84.

Davies-Jones, R., 1984: Streamwise vorticity: The origin of updraft rotation in supercell storms. *J. Atmos. Sci.,* **41,** 2991–3006.

Donaldson, R., R. Dyer, and M. Kraus, 1975: An objective evaluator of techniques for prediction of severe weather events. Preprints, *Ninth Conf. on Severe Local Storms,* Norman, OK, Amer. Meteor. Soc., 321–326.

Doswell, C. A., III, 1987: The distinction between large-scale and mesoscale contribution to severe convection: A case study example. *Wea. Forecasting,* **2,** 3–16.

——, and J. Flueck, 1989: Forecasting and verifying in a field research project: DOPLIGHT '87. *Wea. Forecasting,* **4,** 97–109.

——, R. Davies-Jones, and D. L. Keller, 1990: On summary measures of skill in rare event forecasting based on contingency tables. *Wea. Forecasting,* **5,** 576–585.

Fankhauser, J. C., A. C. Modahl, C. G. Mohr, and M. E. Solak, 1976: *Meteorological Summary.* Vol. III, *Final Report—National Hail Research Experiment Randomized Seeding Experiment 1972–1974,* National Center for Atmospheric Research, 19 pp.

Federer, B., U. Görner, D. Högl, and A. Waldvogel, 1973: Bericht über das Feldexperiment im Bassin Lemanique vom 23. Mai–15. August 1972. Wissenschaftliche Mitteilung 69, Laboratorium für Atmosphärenphysik, ETH, Zürich, Switzerland, 125 pp.

Fuelberg, H. E., and D. G. Biggar, 1994: The preconvective environment of summer thunderstorms over the Florida panhandle. *Wea. Forecasting,* **9,** 316–326.

George, J. J., 1960: *Weather Forecasting for Aeronautics.* Academic Press.

Grosh, R. C., and G. M. Morgan Jr., 1975: Radar-thermodynamic hail day determination. Preprints, *Ninth Conf. on Severe Local Storms,* Norman, OK, Amer. Meteor. Soc., 454–459.

Gruppe für Radarmeteorologie, 1995: Monitoring von starken Hagelstürmen in der Schweiz 1994. LAPETH-33, 243 pp. [Available from Atmospheric Science, ETH, 8093 Zürich, Switzerland.]

Hanssen, A. W., and W. J. A. Kuipers, 1965: On the relationship between the frequency of rain and various meteorological parameters. *Meded. Verhand. K. Nederlands Meteor. Inst.,* **81,** 2–15.

Hart, J. A., and W. D. Korotky, 1991: The SHARP workstation—v1.50. A skew T/hodograph analysis and research program for the IBM and compatible PC: User's manual. NOAA/NWS Forecast Office, Charleston, WV, 62 pp.

Hofmann, A., 1974: Alternativ–Vorhersagen. *Promet,* **4,** 6–7.

Houze, R. A., Jr., B. F. Smull, and P. Dodge, 1990: Mesoscale organization of springtime rainstorms in Oklahoma. *Mon. Wea. Rev.,* **118,** 613–654.

——, W. Schmid, R. G. Fovell, and H.-H. Schiesser, 1993: Hailstorms

in Switzerland: Left movers, right movers, and false hooks. *Mon. Wea. Rev.*, **121,** 3345–3370.

Huntrieser, H., 1995: Zur Bildung, Verteilung und Vorhersage von Gewittern in der Schweiz. Ph.D. thesis, ETH, Zürich, Switzerland, 246 pp. [Available from Atmospheric Science ETH, 8093 Zürich, Switzerland.]

——, H.-H. Schiesser, W. Schmid, and S. Willemse, 1994a: The evolution of the ''mesoscale convective system'' over Switzerland. *The Squall Line of 21 July 1992 in Switzerland and Southern Germany—A Documentation,* S. P. Haase-Straub, D. Heimann, T. Hauf, and R. K. Smith, Eds., Institut für Physik der Atmosphäre, 39–66.

——, ——, and A. Waldvogel, 1994b: The synoptic and mesoscale environment of severe convective activity in Switzerland. *The Life Cycles of Extratropical Cyclones,* Vol. III, Amer. Meteor. Soc., 101–106.

Jacovides, C. P., and T. Yonetani, 1990: An evaluation of stability indices for thunderstorm prediction in greater Cyprus. *Wea. Forecasting,* **5,** 559–569.

Johns, R. H., and C. A. Doswell III, 1992: Severe local storms forecasting. *Wea. Forecasting,* **7,** 588–612.

Lee, R. R., and J. E. Passner, 1993: The development and verification of TIPS: An expert system to forecast thunderstorm occurrence. *Wea. Forecasting,* **8,** 271–280.

Lilly, D. K., 1986: The structure, energetics and propagation of rotating convective storms. Part II: Helicity and storm stabilization. *J. Atmos. Sci.,* **43,** 126–140.

——, 1990: Numerical prediction of thunderstorms—Has its time come? *Quart. J. Roy. Meteor. Soc.,* **116,** 779–798.

Litynska, Z., J. Parfiniewicz, and H. Pinkowski, 1976: The prediction of airmass thunderstorms and hails. *W.M.O. Bull.,* **450,** 128–130.

Maddox, R. A., 1976: An evaluation of tornado proximity wind and stability data. *Mon. Wea. Rev.,* **104,** 133–142.

Mahrt, L., 1977: Influence of low-level environment on severity of High Plains moist convection. *Mon. Wea. Rev.,* **105,** 1315–1329.

McCoy, M. C., 1986: Severe-storm-forecast results from the PROFS 1983 forecast experiment. *Bull. Amer. Meteor. Soc.,* **67,** 155–164.

Means, L. L., 1952: Stability index computation graph for surface data. 2 pp. [Unpublished manuscript available from F. Sanders, 9 Flint St., Marblehead, MA 01945.]

Miller, R. C., 1967: Notes on analysis and severe storm forecasting procedures of the Military Weather Warning Center. AWS Tech. Rep. 200, USAF, 170 pp. [Available from Headquarters, AWS, Scott AFB, IL 62225.]

Modahl, A. C., 1979: Synoptic parameters as discriminators between hailfall and less significant convective activity in northeast Colorado. *J. Appl. Meteor.,* **18,** 671–681.

Moller, A. R., C. A. Doswell, M. P. Foster, and G. R. Woodall, 1994: The operational recognition of supercell thunderstorm environments and storm structures. *Wea. Forecasting,* **9,** 327–347.

Moncrieff, M. W., and M. J. Miller, 1976: The dynamics and simulation of tropical cumulonimbus and squall lines. *Quart. J. Roy. Meteor. Soc.,* **102,** 373–394.

Morris, R. M., 1986: The Spanish plume—Testing the forecaster's nerve. *Meteor. Mag.,* **115,** 349–357.

Mosteller, F., and J. W. Tukey, 1977: *Data Analysis and Regression.* Addison-Wesley, 577 pp.

Mueller, C. K., J. W. Wilson, and N. A. Crook, 1993: The utility of sounding and mesonet data to nowcast thunderstorm initiation. *Wea. Forecasting,* **8,** 132–146.

Neumann, C. J., 1971: The thunderstorm forecasting system at the Kennedy Space Center. *J. Appl. Meteor.,* **10,** 921–936.

Newton, C. W., 1967: Severe convective storms. *Advances in Geophysics,* Vol. 12, Academic Press, 257–303.

Orlanski, I., 1975: A rational subdivision of scales for atmospheric processes. *Bull. Amer. Meteor. Soc.,* **56,** 527–530.

Peppler, R. A., and P. J. Lamb, 1989: Tropospheric static stability and central North American growing season rainfall. *Mon. Wea. Rev.,* **117,** 1156–1180.

Reap, R. M., and D. S. Foster, 1979: Automated 12–36 hour probability forecasts of thunderstorms and severe local storms. *J. Appl. Meteor.,* **18,** 1304–1315.

Rockwood, A. A., and R. A. Maddox, 1988: Mesoscale and synoptic interactions leading to intense convection: The case of 7 June 1982. *Wea. Forecasting,* **3,** 51–68.

Rotunno, R., and J. B. Klemp, 1982: The influence of the shear-induced pressure gradient on thunderstorm motion. *Mon. Wea. Rev.,* **110,** 136–151.

——, and ——, 1985: On the rotation and propagation of simulated supercell storms. *J. Atmos. Sci.,* **42,** 271–292.

Saucier, W. J., 1955: *Principles of Meteorological Analysis.* University of Chicago Press, 438 pp.

Schiesser, H.-H., R. A. Houze Jr., and H. Huntrieser, 1995: The mesoscale structure of severe precipitation systems in Switzerland. *Mon. Wea. Rev.,* **123,** 2070–2097.

Schmid, W., and H. Huntrieser, 1994: The wind environment of supercell storms in Switzerland. *Ann. Meteor.,* **30,** 13–16.

——, L. Li, H. H. Schiesser, and R. A. Houze Jr., 1993: Rotation in Swiss hailstorms: Doppler radar structure and the environmental wind field. Preprints, *17th Conf. on Severe Local Storms,* St. Louis, MO, Amer. Meteor. Soc., 196–200.

Schultz, P., 1989: Relationships of several stability indices to convective weather events in northeast Colorado. *Wea. Forecasting,* **4,** 73–80.

Showalter, A. K., 1953: A stability index for thunderstorm forecasting. *Bull. Amer. Meteor. Soc.,* **34,** 250–252.

Stackpole, J., 1967: Numerical analysis of atmospheric soundings. *J. Appl. Meteor.,* **6,** 464–467.

Steinacker, R., 1977: Möglichkeiten von Gewitterprognosen im Gebirge. *Wetter Leben,* **29,** 150–156.

Stone, H. M., 1985: A comparison among various thermodynamic parameters for the prediction of convective activity. NOAA Tech. Memo. NWS ER-68, NWS Eastern Region, Garden City, NY, 14 pp. [NTIS PB85-206 217/AXB.]

Weisman, M. L., and J. B. Klemp, 1982: The dependence of numerically simulated convective storms on vertical wind shear and buoyancy. *Mon. Wea. Rev.,* **110,** 504–520.

——, and ——, 1984: The structure and classification of numerically simulated convective storms in directionally varying wind shears. *Mon. Wea. Rev.,* **112,** 2479–2498.

Wilson, J. W., and W. E. Schreiber, 1986: Initiation of convective storms at radar-observed boundary layer convergence lines. *Mon. Wea. Rev.,* **114,** 2516–2536.

TABLE A1. Summary of thermodynamic and kinematic parameters used: T is temperature (°C), T_d is dewpoint temperature (°C), Θ is potential temperature (K), Θ_e is equivalent potential temperature (K), ρ is density (kg m^{-3}), g is the acceleration of gravity (m s^{-2}), z is height (m), H is height of an indicated pressure level (decameter), ν is wind speed (m s^{-1}), and S is vertical wind shear between two indicated levels (s^{-1}). Subscripted numbers indicate constant pressure levels.

Parameter	Code	Key reference(s)	Equation	Explanation
Category A: Stability indices				
K	K	George (1960)	$K = T_{850} - T_{500} + T_{d850} - (T_{700} - T_{d700})$	Notation as given above
Total totals	TT	Miller (1967)	$TT = (T_{850} - T_{500})2 - T_{850} + T_{d850}$	Notation as given above
Showalter	SI_{850}	Showalter (1953)	$SI_{850} = T_{500} - T'_{850hPa \rightarrow 500hPa}$	$T'_{850hPa \rightarrow 500hPa}$ is the 500-hPa temperature of a parcel lifted dry adiabatically from 850 hPa to its condensation level and moist adiabatically thereafter
Modified Showalter	SI_{700}	Steinacker (1977)	$SI_{700} = T_{500} - T'_{700hPa \rightarrow 500hPa}$	Same as SI_{850} except initial parcel is lifted from 700 hPa
Modified Showalter	SI_{CCL}	—	$SI_{CCL} = T_{500} - T'_{CCL \rightarrow 500hPa}$	$T'_{CCL \rightarrow 500hPa}$ is the 500-hPa temperature of a parcel lifted moist adiabatically from its modified convective condensation level CCL_{MOD} (as defined below)
Modified Showalter	SI_{LCL}	—	$SI_{LCL} = T_{500} - T'_{LCL \rightarrow 500hPa}$	$T'_{LCL \rightarrow 500hPa}$ is the 500-hPa temperature of a parcel lifted moist adiabatically from its modified lifted condensation level LCL_{MOD} (as defined below)
Surface lifted	SLI	Means (1952)	$SLI = T_{500} - T'_{Surface \rightarrow 500hPa}$	Same as SI_{850} except initial parcel is lifted from the surface
Deep convective	DCI	Barlow (1993)	$DCI = (T + T_d)_{850} - SLI$	Notation as given above
Humidity	HI	Litynska et al. (1976)	$HI = (T - T_d)_{850} + (T - T_d)_{700} + (T - T_d)_{500}$	Notation as given above
Boyden	BI	Boyden (1963)	$BI = H_{700} - H_{1000} - T_{700} - 200$	Notation as given above
KO	KO	Andersson et al. (1989)	$KO = \frac{(\Theta_{e500} + \Theta_{e700} - \Theta_{e1000} - \Theta_{e850})}{2}$	Notation as given above
Severe weather threat	SWEAT	Bidner (1971)	$SWEAT = 12T_{d850} + 20(TT - 49) + 4\nu_{850} + 2\nu_{500} + 125S_{850hPa \rightarrow 500hPa}$	Notation as given above
Category B: Energy and shear indices				
Convective available potential energy	$CAPE_{Surface}$	Moncrieff and Miller (1976)	$CAPE_{Surface} = g \int_{\Theta \geq \Theta'} \frac{\Theta(z) - \Theta'(z)}{\Theta'(z)} dz$	$\Theta(z)$ is the potential temperature of a parcel lifted dry adiabatically from the surface to its condensation level and moist adiabatically thereafter $\Theta'(z)$ is the potential temperature of the environment
Modified convective available potential energy	$CAPE_{850}$	—	$CAPE_{850hPa} = g \int_{\Theta \geq \Theta'} \frac{\Theta(z) - \Theta'(z)}{\Theta'(z)} dz$	Same as $CAPE_{Surface}$ except initial parcel is lifted from 850 hPa
Modified convective available potential energy	$CAPE_{CCL}$	—	$CAPE_{CCL} = g \int_{\Theta \geq \Theta'} \frac{\Theta(z) - \Theta'(z)}{\Theta'(z)} dz$	Same as $CAPE_{Surface}$ except initial parcel is lifted moist adiabatically from its modified convective condensation level CCL_{MOD} (as defined below)

TABLE 1. (*Continued*).

Skill score	Code	Reference(s)	Equation	Limits
Modified convective available potential energy	$CAPE_{LCL}$	—	$CAPE_{LCL} = g \int_{\Theta \geq \Theta'} \frac{\Theta(z) - \Theta'(z)}{\Theta'(z)}\, dz$	Same as $CAPE_{Surface}$ except initial parcel is lifted moist adiabatically from its modified lifted convective condensation level LCL_{MOD} (as defined below)
Bulk Richardson number	Ri	Weisman and Klemp (1982, 1984)	$Ri = \frac{CAPE}{\frac{1}{2}[S^2]}$	Notation as given above and below
Vertical wind shear	S	Weisman and Klemp (1982, 1984)	$S = \frac{\int_0^{6\ km} \rho(z)\lvert\nu(z)\rvert\, dz}{\int_0^{6\ km} \rho(z)\, dz} - \frac{1}{2}\lvert\nu(0) + \nu(0.5\ km)\rvert$	Here S is the average density-weighted wind shear in the layer 0.5–6 km
Category C: Cloud-based heights				
Convective condensation level	CCL	Saucier (1955) Stackpole (1967)	—	Used by thermal thunderstorm initiation, CCL is where the surface mixing ratio line intersects the temperature curve
Modified convective condensation level	CCL_{MOD}	Federer et al. (1973)	—	CCL_{MOD} is where the mean mixing ratio line between the surface and 850 hPa intersects the temperature curve
Lifted condensation level	LCL	Saucier (1955) Stackpole (1967) Bolton (1980)	—	Used by frontal thunderstorm initiation, LCL is where the surface mixing ratio line intersects the surface dry adiabate
Modified lifted condensation level	LCL_{MOD}	Fankhauser et al. (1976)	—	LCL_{MOD} is where the mean mixing ratio line of the lowest 50 hPa intersects with the mean dry adiabate of the lowest 50 hPa